ORIGINAL RESEARCH ARTICLE

Fatal lymphocytic cardiac damage in coronavirus disease 2019 (COVID-19): autopsy reveals a ferroptosis signature

Werner Jacobs[1,2], Martin Lammens[3], Annelies Kerckhofs[1], Evy Voets[4], Emily Van San[5,6], Samya Van Coillie[5,6], Cédric Peleman[7,8], Matthias Mergeay[4], Sabriya Sirimsi[3], Veerle Matheeussen[9], Hilde Jansens[9], Ingrid Baar[10], Tom Vanden Berghe[5,6,7,11] and Philippe G. Jorens[7,8,10]* (iD)

[1]Department of Forensic Medicine, Antwerp University Hospital, University of Antwerp, Edegem, Belgium; [2]Military Hospital Queen Astrid, Crisis Unit, Belgian Defense, Brussels, Belgium; [3]Department of Pathology, Antwerp University Hospital, University of Antwerp, Edegem, Belgium; [4]Department of Anesthesia and Critical Care Medicine, General Hospital Sint Dimpna, Geel, Belgium; [5]VIB Center for Inflammation Research, Ghent, Belgium; [6]Department of Biomedical Molecular Biology, Ghent University, Ghent, Belgium; [7]Infla-Med Research Consortium of Excellence, University of Antwerp, Antwerp, Belgium; [8]Department of Medicine and Health Sciences, Laboratory of Experimental Medicine and Pediatrics (LEMP), University of Antwerp, Antwerp, Belgium; [9]Department of Microbiology, Central Laboratory, Antwerp University Hospital, University of Antwerp, Edegem, Belgium; [10]Department of Intensive Care Medicine, Antwerp University Hospital, University of Antwerp, Wilrijkstraat 10, Edegem, B-2650, Belgium; [11]Department of Biomedical Sciences, University of Antwerp, Antwerp, Belgium

Abstract

Aims Cardiovascular complications, including myocarditis, are observed in coronavirus disease 2019 (COVID-19). Major cardiac involvement is a potentially lethal feature in severe cases. We sought to describe the underlying pathophysiological mechanism in COVID-19 lethal cardiogenic shock.

Methods and results We report on a 48-year-old male COVID-19 patient with cardiogenic shock; despite extracorporeal life support, dialysis, and massive pharmacological support, this rescue therapy was not successful. Severe acute respiratory syndrome coronavirus 2 RNA was detected at autopsy in the lungs and myocardium. Histopathological examination revealed diffuse alveolar damage, proliferation of type II pneumocytes, lymphocytes in the lung interstitium, and pulmonary microemboli. Moreover, patchy muscular, sometimes perivascular, interstitial mononuclear inflammatory infiltrates, dominated by lymphocytes, were seen in the cardiac tissue. The lymphocytes 'interlocked' the myocytes, resulting in myocyte degeneration and necrosis. Predominantly, T-cell lymphocytes with a CD4:CD8 ratio of 1.7 infiltrated the interstitial myocardium, reflecting true myocarditis. The myocardial tissue was examined for markers of ferroptosis, an iron-catalysed form of regulated cell death that occurs through excessive peroxidation of polyunsaturated fatty acids. Immunohistochemical staining with E06, a monoclonal antibody binding to oxidized phosphatidylcholine (reflecting lipid peroxidation during ferroptosis), was positive in morphologically degenerating and necrotic cardiomyocytes adjacent to the infiltrate of lymphocytes, near arteries, in the epicardium and myocardium. A similar ferroptosis signature was present in the myocardium of a COVID-19 subject without myocarditis. In a case of sudden death due to viral myocarditis of unknown aetiology, however, immunohistochemical staining with E06 was negative. The renal proximal tubuli stained positively for E06 and also hydroxynonenal (4-HNE), a reactive breakdown product of the lipid peroxides that execute ferroptosis. In the case of myocarditis of other aetiology, the renal tissue displayed no positivity for E06 or 4-HNE.

Conclusions The findings in this case are unique as this is the first report on accumulated oxidized phospholipids (or their breakdown products) in myocardial and renal tissue in COVID-19. This highlights ferroptosis, proposed to detrimentally contribute to some forms of ischaemia–reperfusion injury, as a detrimental factor in COVID-19 cardiac damage and multiple organ failure.

Introduction

The ongoing severe acute respiratory syndrome coronavirus 2 (SARS-CoV-2) pandemic is responsible for a great many cases of respiratory syndrome coronavirus disease 2019 (COVID-19), which is characterized by respiratory distress with radiological and clinical features resembling full-blown acute respiratory distress syndrome (ARDS).[1] Recently, attention has been drawn to the cardiac complications of this disease. Amongst hospitalized COVID-19 patients, some form of cardiac injury is seen in up to 27,8 %,[2] as evidenced by a rise in cardiac troponin I (TnI) serum levels.[2] Major cardiac involvement is a potentially lethal feature in severe COVID-19.

Fulminant myocarditis, an acute rapidly progressive form of myocardial failure caused by infectious and non-infectious agents and in systemic diseases, is characterized and accompanied by marked inflammation and has a poor in-hospital outcome.[3] The diagnosis of fulminant myocarditis is based on clinical suspicion and can be confirmed by endomyocardial biopsy. In view of the marked inflammation seen in COVID-19 patients and the apparently very poor prognosis of cardiac failure in young patients, myocarditis rather than ischaemic cardiogenic shock has been proposed as the underlying mechanism in some cases of COVID-19 related cardiac injury; nevertheless, there is little published data about the underlying pathologic mechanisms that might cause this type of cardiac failure to occur in COVID-19 patients.

Case report

On 21 March 2020, a 48-year-old man presented at a regional hospital with a 7-day history of fever, diarrhoea, cough, dysosmia, and dyspnoea. His medical history was uneventful apart from hypertension, for which he took an angiotensin II receptor blocker daily. Initially, oxygen saturation was 87% without oxygen, and his body temperature was 38.6°C; the electrocardiogram revealed no abnormalities. Rapidly progressive shortness of breath and hypoxaemia necessitated intubation within hours, as well as prone ventilation to achieve sufficient oxygenation, which at that time resulted in a decline in the amount of oxygen needed (FiO$_2$ of 55%). Polymerase chain reaction on both the nasopharyngeal aspirate and a throat swab was positive for SARS-CoV-2 RNA. Other viruses (cytomegalovirus, herpes simplex virus, adenovirus, and parainfluenza virus) were also tested for but turned out negative. A chest computed tomography showed typical pneumonia, as seen in COVID-19 infection (*Figure 1A*). Hydroxychloroquine and azithromycin were administered. Rapidly progressive acute kidney injury with anuria necessitated continuous venovenous hemofiltration. Lung protective ventilation in an airway pressure release ventilation mode was applied. In the afternoon of Day 12 of its illness, 5 days after hospital admission (26 March), there was a rapidly progressive lactic acidosis and shock, necessitating vasopressors and inotropics (noradrenaline, adrenaline, and dobutamine). Laboratory tests showed an increase of the troponin I level from 12.1

FIGURE 1 (A) Chest CT. The coronal image shows multiple patchy ground-glass opacifications in all lung fields (right more than left) (Illness Day 7, Hospital Day 1). (B) Electrocardiogram on Day 5 after admission showing a widened QRS in the absence of hypokalaemia (Illness Day 11, Hospital Day 5).
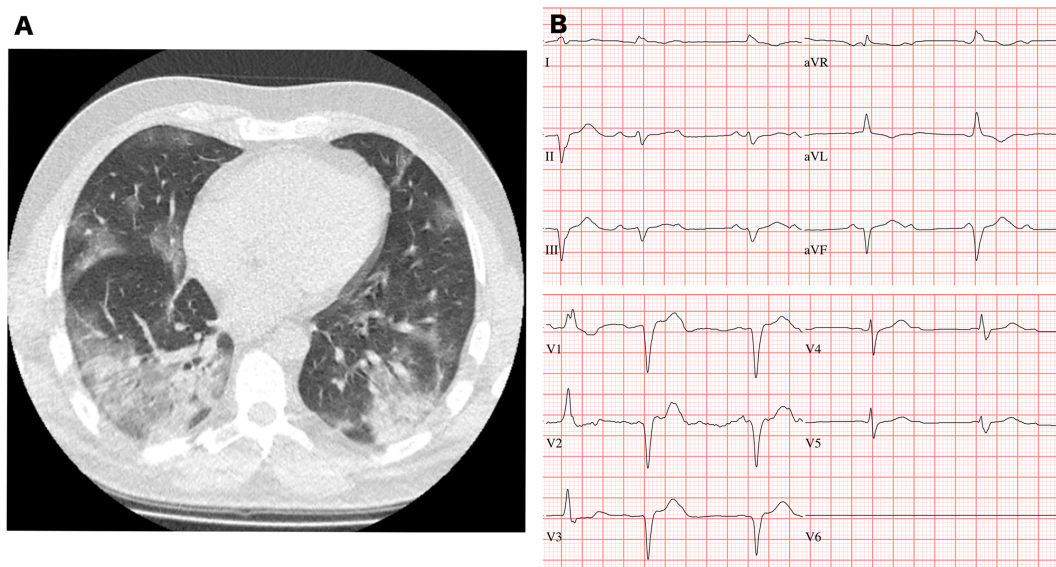
on admission to 14 932 ng/L (normal value < 45 ng/L) (*Table 1*). Echocardiography showed a hyperdynamic ventricular function, although under massive support of inotropic agents and vasopressors. No significant valvular pathology was seen. Pulmonary pressures could not be measured (in absence of a tricuspid insufficiency). An interventricular septum dimension of 12 mm and posterior wall dimension of 11 mm were noted. The left ventricular end diastolic diameter was 48 mm. There was no pericardial effusion. His lymphocyte count had been low at admission (300 μL^{-1}) and remained low during the whole hospitalization (*Table 1*). Broad-spectrum antibiotics were added to cover sepsis, and hydrocortisone 100 mg t.i.d. was administered in view of the massive shock. Electrocardiography findings showed marked QRS widening and a positive deflection at the end of the T wave in the absence of hypokalaemia (*Figure 1B*). Given the suspicion of myocarditis and the deep shock, venoarterial extracorporeal membrane oxygenation was installed on the scene by the extracorporeal membrane oxygenation team of the Antwerp University Hospital; the patient was then transported by this team to the intensive care unit of this tertiary referral hospital. At this time, the patient's ferritin levels were massively elevated: the initial level of 1200 μg/L rose up to 32 401 μg/L (normal value < 322 μg/L) and was accompanied by severe hypertriglyceridaemia (481 mg/dL, normal < 120 mg/dL). The serum interleukin 6 level was 281 pg/mL (normal < 7 pg/mL). The N terminal pro brain natriuretic peptide level as a marker of cardiac failure was 9223 pg/mL (normal < 125 pg/mL). Culture of endotracheal aspirate and blood cultures in both hospitals did not reveal any accompanying bacterial infection. Despite the extracorporeal life support, dialysis, and massive pharmacological support, this rescue therapy was not successful: there was an absence of any pulsatility in the arterial waveform, and the patient died due to refractory shock on 27 March 2020.

As there is a dearth of published pathology data on the underlying physiopathology of organ failure and death in COVID-19 are similarly lacking, a clinical autopsy was performed after receiving permission from the patient's family.

External examination showed an overweight adult male patient. Citrine-coloured pleural fluid was present in both thoracic cavities. The lungs (left 1498 g, right 1635 g) were purplish, edematous, with a mottled aspect (*Figure 2A*). The pericardial sac was filled with yellow citrine-coloured fluid. The heart was hypertrophic (605 g) with widened right and left ventricles and thickened ventricle walls (left 15 mm, septum 14 mm, and right 6 mm). On the outer wall of the left ventricle and the endocardium, some petechiae were noticed (*Figure 2B*). The coronaries were perfectly passable without atherosclerosis. The cut surface did not show macroscopic particularities. Ascites fluid was present in the abdominal cavity. The kidneys showed signs of acute kidney injury. The spleen (358 g) showed multiple infarctions without thromboemboli.

Microscopically, diffuse alveolar damage with intra-alveolar and interstitial oedema and denudation of the alveolar epithelium with hyaline membrane formation was observed in both lungs, indicating ARDS. Re-epithelialization with proliferation of type II pneumocytes was also found in several zones (*Figure 3*). Multinucleated cells were also identified (Supporting Information, *Figure S1*). The epithelial cells showed striking reactive cytonuclear changes with polymorphic nuclei and prominent nucleoli. No obvious intranuclear or intracytoplasmic viral inclusions were identified. Interstitially, there were diffuse inflammatory infiltrates, dominated by lymphocytes. Only mild neutrophilic inflammation was present. We also report on multiple peripheral pulmonary arterial microemboli in both lungs (*Figure 3*, insert), which might reflect the procoagulant profile as well as microangiopathy seen in COVID-19 patients making them prone to thromboembolic complications in large as well as small alveolar capillary vessels.[4]

Histopathological examination showed hypertrophic cardiac tissue with patchy muscular, sometimes perivascular, and slightly diffuse interstitial mononuclear inflammatory infiltrates, dominated by lymphocytes (*Figure 4*). No thrombotic events were observed in the microcirculation of the heart. In the patchy areas, the lymphocytes 'interlocked' the myocytes, resulting in myocyte degeneration and necrosis (piecemeal necrosis). Intermingled with lymphocytes, only a very few individual polymorphous neutrophils were found in the affected areas. Signs of inflammation were present in both the epicardium and the myocardium. By immunohistochemistry, the lymphocytes were positive with CD3, CD4, CD8, and a small number of CD20. In the largest inflammatory infiltrate, 92% of the lymphocytes were CD3 + T

Table 1 Evolution of laboratory results

	21.03.20	22.03.20	23.03.20	24.03.20	25.03.20	26.03.20	27.03.20	Normal values
WBC (×10^3/μL)	10.6	12.5	25.6	19.4	11.0	12.4	14.6	3.9–10.6
Lymphocytes (×10^3/μL)	0.30	0.26	0.26	0.35	MD	0.45	0.77	1.00–4.80
D-dimers (μg/L)	611	MD	MD	MD	MD	MD	MD	0–549
Troponin I (ng/L)	12.1	12.2	143.2	97.7	59.2	108.4	14 932	0.0–34.2
CRP (mg/L)	247.1	340.9	462	547.7	472.5	441.9	318	<5.0
Ferritin (μg/L)	1200	MD	MD	MD	MD	MD	32 401	<322
INR	MD	MD	1.06	1.04	1.05	1.15	1.15	0.9–1.2

CRP, C-reactive protein; INR, international normalized ratio; MD, missing values; WBC, white blood cells.

FIGURE 2 Macroscopy at autopsy. (A) The lungs were purplish, edematous, and had a mottled aspect. (B) View on the left ventricle with some petechiae in the endocardium.
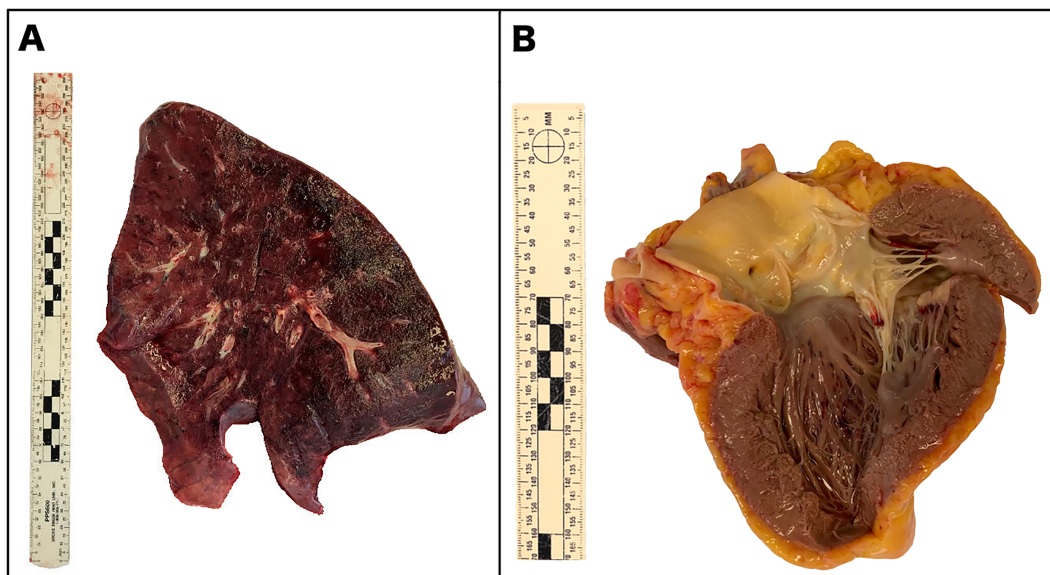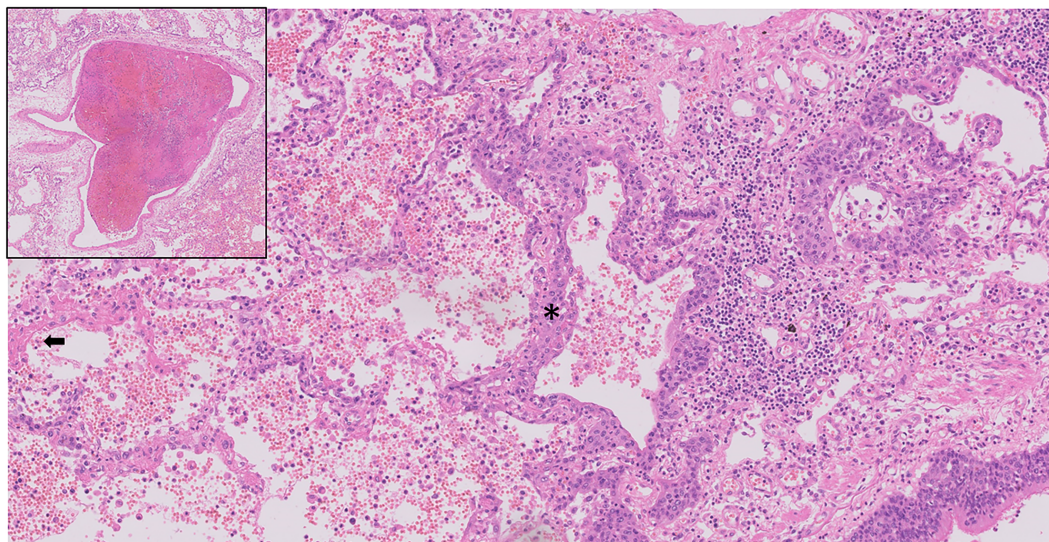

FIGURE 3 Lung tissue with diffuse alveolar damage, with hyaline formation (arrow), marked type 2 pneumocyte hyperplasia (asterisk) with prominent nucleoli and multinucleation and interstitial mononuclear inflammatory infiltrates (predominantly with lymphocytes) (original magnification ×100). Insert: microembolus.

lymphocytes, and 8% were CD20 + B lymphocytes. The CD4: CD8 ratio was 1.7. These findings indicate a predominant T-cell phenotype of the cardiac inflammatory infiltrate. Intermingled, there was limited number of CD68-positive macrophages. CD138 showed a few plasma cells. As no interstitial fibrosis disarray of the muscle fibres was seen, true preexisting cardiomyopathy could be excluded.

The spleen showed a disturbed architecture with multiple recently infarcted zones without thromboemboli. In the kidneys, a striking amount of intratubular oxalate crystals was found. There was also a slight presence of interstitial inflammation in the kidneys and signs of acute tubular necrosis. Furthermore, organ damage in the liver was observed in the context of shock.

FIGURE 4 Histochemical and immunohistochemical examination of a heart tissue sample (several sections of the heart performed: septum *n* = 2, anterior wall *n* = 2, posterior wall *n* = 2, right ventricle *n* = 1). Lymphocytes infiltrating the cardiomyocytes (A–C), resulting in myocyte degeneration and necrosis (D). Most of the lymphocytes are CD3-positive (B) and CD4-positive (C) T-cells. The CD4-positive cells progressively infiltrate the cardiomyocytes (C) demonstrated by the progressive disappearance of the desmin-positive myofibrils (brown in panel D) and are accompanied with only a few CD68-positive macrophages (E). Staining: HE (A), CD3 (B), CD4 (C), desmin (D), and CD68 (E). Original magnification: ×50 (A, B) and ×200 (C, D).
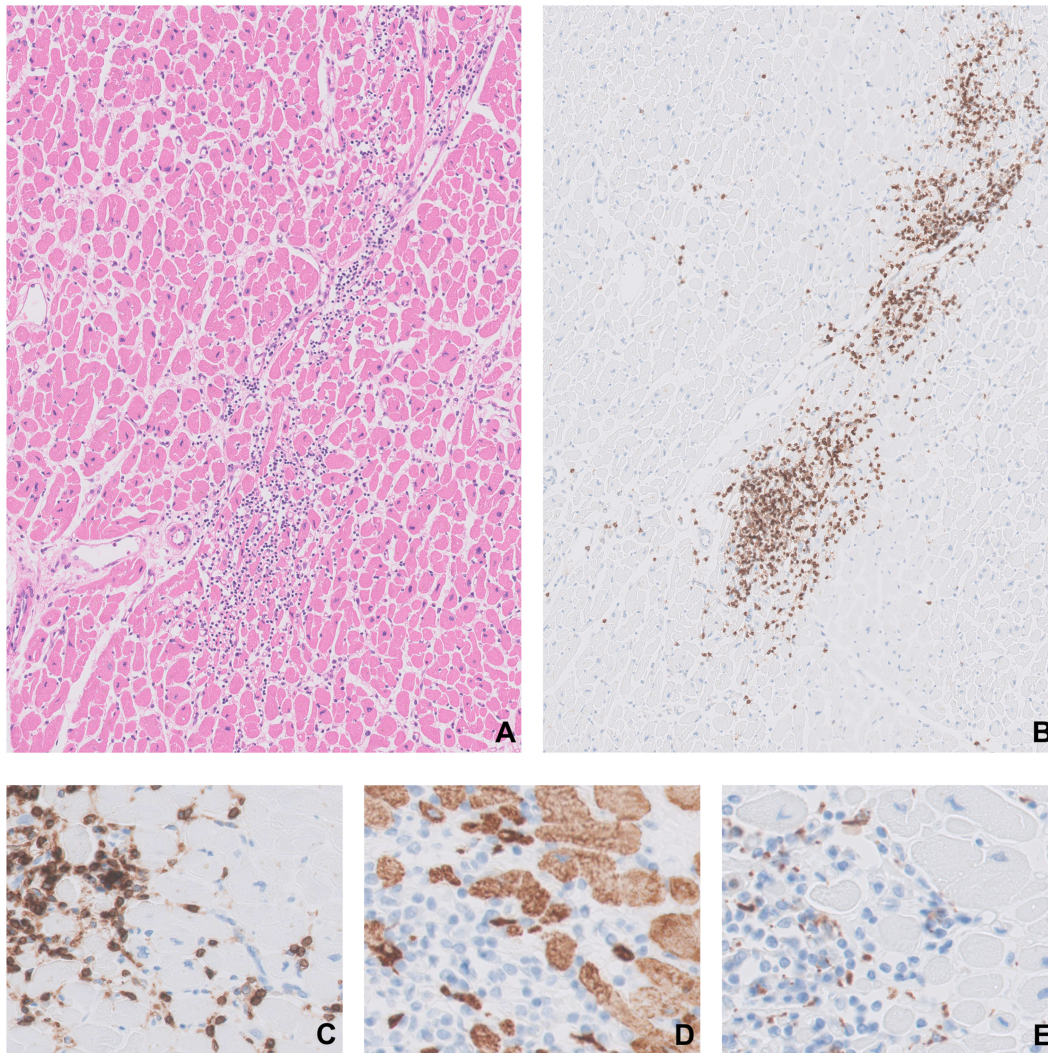
Molecular detection of SARS-CoV-2 in the samples (heart and lung biopsy, endotracheal and nasopharyngeal aspirate) was done by targeting the SARS-CoV-2 envelope (E)-gene according to a World Health Organization recommended protocol.[5] The cycle threshold (Ct) value for the E-gene and corresponding viral load (log10 RNA copies/mL) were 28.94/5.6 (nasopharyngeal aspirate), 31.22/4.9 (endotracheal aspirate), 23.44/7.4 (lung biopsy), 35.90/3.5 (pericardial swab), and 31.53/4.9 (heart biopsy). Additional confirmatory testing was performed on the heart biopsy by targeting the SARS-CoV-2 nucleocapside (N) gene according to the Centers for Disease Control and Prevention protocol (N1 and N3).[6] The

Ct values for the N-gene in the heart biopsy were 31.74 (N1) and 31.64 (N3).

Ferroptosis signature

We examined the patient's myocardial tissue for markers of ferroptosis, an iron-catalysed form of regulated cell death that occurs through excessive peroxidation of polyunsaturated fatty acids and is also proposed to detrimentally contribute to some forms of ischaemia–reperfusion injury,

stroke, and degenerative diseases.[7] Immunohistochemical staining with E06 (*Figure 5A*), a monoclonal antibody binding to oxidized phosphatidylcholine (reflecting lipid peroxidation during ferroptosis), was positive in morphologically degenerating and necrotic cardiomyocytes adjacent to the infiltrate of lymphocytes.[8,9] E06 positivity was also found near arteries, in the epicardium and myocardium. Note a gradient-like staining, reflecting a wave of synchronized necrosis, as has been reported to occur for ferroptosis.[10] This specific myocardial immunodetection of abundant lipid peroxides with E06 antibody was replicated several times on independent staining procedures. Of note, in a case of sudden death due to viral myocarditis of unknown aetiology, immunohistochemical staining with E06 was negative (*Figure 5B*). The hypertrophic myocardium of a deceased COVID-19 patient with severe ARDS, but without cardiac failure/myocarditis, showed only small foci of E06 positivity throughout the ventricular wall (*Figure 5C*). The myocardium, also obtained at autopsy, of a COVID-19 subject without myocarditis (after sudden death due to trauma) did not show this prominent signature for E06 (*Figure 5D*).

In order to elucidate the role of ferroptosis during multiple organ dysfunction syndrome (MODS)[11] including cardiac and renal failure in this patient, immunohistochemical staining was performed on renal tissue using E06 and anti-4-hydroxynonenal (HNE) antibody. 4-HNE is a highly reactive breakdown product of the lipid peroxides that execute ferroptosis.[11] Renal tissue of the COVID-19 patient with lymphocytic myocarditis stained positively for both E06 and 4-HNE in the cortical region. More precisely, these ferroptosis markers are detected in the proximal tubuli (*Figures 6A* and *6C*). In the case of sudden death due to myocarditis of other aetiology, the morphologically normal renal tissue displayed no positivity for E06 or 4-HNE (*Figures 6B* and *6D*, respectively). Attempts to stain lung tissue failed due to high background staining from multiple lung haemorrhages.

Discussion

At the time of writing, there are few published autopsy findings in COVID-19 patients, where damage mostly of the lungs is reported but not of the heart tissue.[12–14] It was described that a few mononuclear cells had infiltrated the interstitium of the heart.[14,15] Viral particles and low-grade interstitial inflammation with vacuolated CD68-positive macrophages were observed in the endomyocardial biopsy of patients with COVID-19 related cardiogenic shock.[15–17] Recently, (low loads of) SARS-COV-2 genomes have been detected in the

FIGURE 5 Immunohistochemical examination of heart tissue for a ferroptosis marker. E06 immunoreactivity (protocol adapted from Haider et al.[9]) was detected in the area of severe SARS-CoV-2 myocarditis, near arteries and throughout the myocardium in a gradient-like manner (A). In a case of a 16-year-old man who suddenly died of non-COVID-19 myocarditis due to other aetiology, no signal was detected on staining with E06 (B). The myocardium of a 33-year-old male COVID-19 patient that succumbed to severe acute respiratory distress syndrome and multiple organ failure, but without myocarditis, showed foci of E06 positivity in all areas of the ventricular wall and perivascular regions (C). The myocardium of another control subject without myocarditis, a 48-year-old man who was hospitalized after trauma, showed only some E06 positivity in perivascular connective tissue (D). Control stains using only secondary antibodies are available in the Supporting Information.
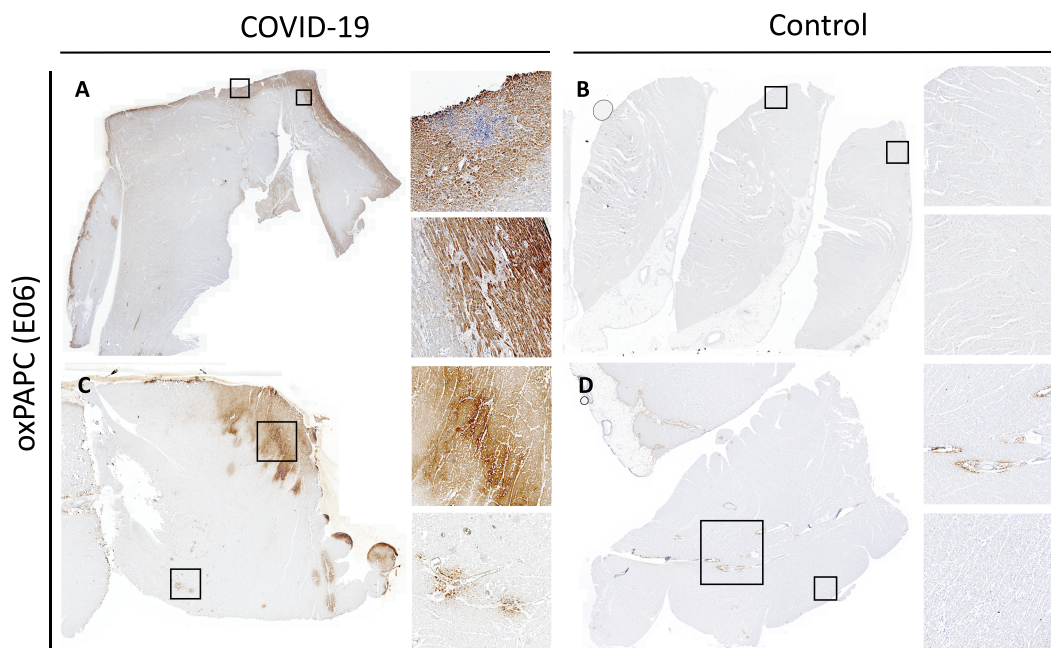
FIGURE 6 Immunohistochemical examination of renal tissue for potential ferroptosis markers. Renal tissue from the COVID-19 patient with myocarditis and multiple organ dysfunction syndrome showed morphological signs of acute tubular necrosis, intratubular oxalate crystals, as well as E06 positivity in proximal tubuli (A). The latter also stained positively for the presence of 4-HNE, one of the breakdown product of lipid peroxides (protocol adapted from Feng et al.[11]) (C). By comparison, in the case of sudden death due to myocarditis of other aetiology, immunohistochemical staining with E06 (B) and anti-4-HNE antibody (D) in the renal tissue showed no presence of these ferroptosis markers (non-specific staining in the corticomedullary junction is also present on control stains). Control stains using only secondary antibodies are enclosed in the Supporting Information.
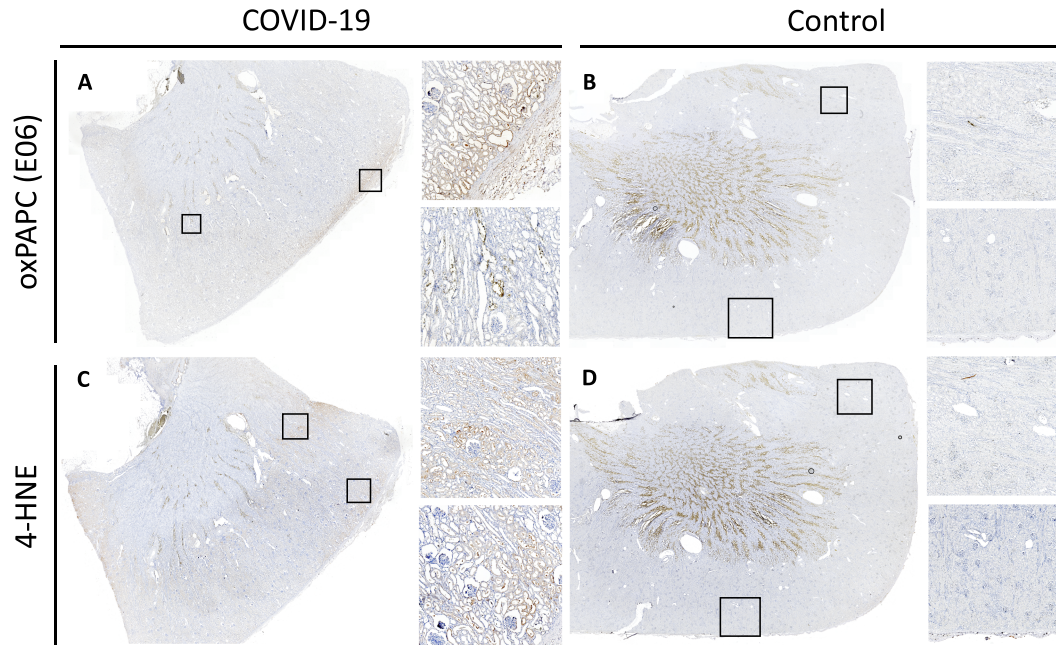
endomyocardial biopsies of 5 out of 104 patients with suspected myocarditis or unexplained heart failure.[18] In one patient, histological analysis revealed an active myocarditis with vessels involved in the inflammation process and accompanying necrosis of myocytes; in the four others, predominantly, T-cells (as stained by a CD3 antibody) were found.[18]

We provide the first in-depth histopathological description of a histology-proven fatal case of SARS-CoV-2 viral myocarditis in a COVID-19 patient with cardiogenic shock together with overt respiratory failure. The findings fulfil the histological, immunohistochemical, and microbiological criteria for definite lymphocytic, myocarditis of viral origin: interstitial, principally CD3-positive, T-lymphocytic infiltration associated with myocyte damage.[19] The COVID-19 causality is supported by reverse transcriptase polymerase chain reaction amplification of the viral genome in myocardial tissue. Moreover, lymphocytes are hardly found in the myocardium of patients dying of septic shock, therefore supporting that the cardiac damage seen in this patient is most probably due to lymphocytic myocarditis; in the case of full-blown septic myocarditis, polynuclear granulocytes would be present. The diagnosis in several previous case reports on fulminant myocarditis due to COVID-19 has been based on clinical signs only.[20,21]

Our data give a unique insight into the physiopathogenesis of COVID-19 related cardiac failure and MODS. The immunohistochemical marker (presence of oxidized phosphatidylcholine) for ferroptosis was positive in myocardial tissue from this COVID-19 related lymphocytic myocarditis and of a case of fatal COVID-19 without myocarditis. Indeed, this COVID-19 patient with lymphocytic myocarditis presented also with refractory shock and multiple organ dysfunction necessitating renal replacement therapy. Microscopically, the renal tissue too displayed signs of acute tubular necrosis, intratubular oxalate crystals, and abundant presence of oxidized phosphatidylcholine and also 4-HNE in the proximal tubules.

Ferroptosis has been conceptualized in 2012 as a novel type of regulated cell death.[22] This form of regulated necrotic cell death is mediated by iron-catalysed lipid peroxides that compromise the plasma membrane integrity. The abundance of lipid peroxides in myocardium and renal cortex of the COVID-19 patient with lymphocytic myocarditis might also be related to ischaemia and ischaemia–reperfusion injury in these organs as seen in MODS.[7,10] Indeed, such insults cause an increased production of radical oxygen species by, for example, the mitochondrial respiratory chain that could subsequently attack polyunsaturated fatty acids, leading to lipid peroxides that execute ferroptosis. In preclinical models, ferroptosis has been implicated in ischaemia–reperfusion injury of the myocardium, kidney, liver, intestine, and brain.[10] Based on our data, it is tempting to suggest that ferroptosis is a detrimental factor in organ injury during shock and MODS

and COVID-19 lymphocytic myocardial infiltration. The cardiac damage observed in the heart might therefore be multifactorial, related to direct invasion of the virus, acid–base imbalance due to kidney injury, hypoxaemia due to respiratory failure as well as ischaemia–reperfusion related ferroptosis due to the severe cardiogenic shock.

Severe acute respiratory syndrome coronavirus 2 was detected in the heart of 35% of those that died from SARS,[23] with the authors concluding that coronaviruses such as SARS-CoV are able to infect and invade the myocardium. At that time, myocardial inflammation caused by SARS-CoV was believed to be predominantly mediated by macrophages,[23] while we additionally show a prominent role for T-lymphocytes in COVID-19. In SARS-infected human cases, marked production of oxidized phospholipids in the inflammatory exudates lining the injured air spaces, pneumocytes, and alveolar macrophages had already been shown,[24] as we show here too in the myocardium and renal tissue as part of the ferroptosis process.

In this patient, as in many other COVID-19 patients with or without myocarditis, extreme hyperferritinemia accompanied by a cytokine 'storm' was seen.[25] Likewise, the patient's myocardial tissue showed an increased signal for ferritin especially in the epicardial region (data not shown). Ferritin is known to be a pro-inflammatory mediator inducing expression of pro-inflammatory molecules[26]; the high ferritin levels observed in these uncommon clinical conditions (sepsis, myocarditis, etc.) are therefore not just the product of the inflammation but rather may contribute to the development of a cytokine storm therefore considered a form of 'hyperferritinemic syndrome'.[27] Our group (and others) has shown that exuberant ferroptosis produces high amounts of ferrous iron that could exceed the buffering capacity of ferritin.[28] The unbuffered, free ferrous iron catalyses radical oxygen species via Fenton reactions and hence lipid peroxides. Along with the cytokine storm and inflammation, this iron dysbiosis might thus also contribute to the hyperferritinemia observed in severe COVID-19 patients. It has been noted that iron dysbiosis, including an increase in plasma ferrous iron and ferritin, also associates with death in critically ill patients with severe acute kidney injury.[29]

In view of the absence of any superimposed infection, fulminant myocarditis was retained as the most plausible diagnosis. More studies are needed to estimate the incidence of SARS-CoV-2 viral myocarditis, although a definite diagnosis on clinical—rather than pathological—data will remain difficult. In an era of high-tech medicine, the autopsy still plays an important role in unravelling the pathophysiology of emerging infectious diseases. In anticipation of the development of effective antiviral therapy, the attenuation of the cytokine storm (e.g. with interleukin 6 receptor blockers) is currently being studied; it remains to be determined if ferroptosis inhibition alone might also be helpful in the treatment of SARS-CoV-2 organ failure, including viral myocarditis.

Highly potent ferroptosis inhibitors might be promising leads for clinical validation.[30]

Conflict of interest

The findings and conclusions in this report are those of the authors. The authors have nothing to disclose.

Author contributions

W.J., M.L., T.V.B., and P.G.J. had full access to all of the data in the study and take responsibility for the integrity of the data and the accuracy of the data analysis. W.J., M.L., A.K., E.V., C.P., T.V.B., and P.G.J. worked on the study concept and design. W.J., M.L., A.K., E.V., E.V.S., S.V.C., C.P., M.M., S.S., V.M., H.J., I.B., T.V.B., and P.G.J. acquired, analysed, or interpreted the data. W.J., M.L., A.K., C.P., T.V.B., and P.G.J. drafted the manuscript. W.J., M.L., A.K., E.V., E.V.S., S.V.C., S.S., V.M., H.J., T.V.B., and P.G.J. provided administrative, technical, or material support. M.L., T.V.B., and P.G.J. supervised the study. All authors contributed to the critical revision of the manuscript for important intellectual content.

Biobank

All samples were stored in the 'Biobank Antwerpen' BE 71030031000; Biobank Antwerpen, BBMR-ERIC, Belgian Virtual Tumourbank funded by the National Cancer Plan; No. Access: (BB20039), Last: (04, 15, 2020) [BIORESOURCE].

Supporting information

Additional supporting information may be found online in the Supporting Information section at the end of the article.

Figure S1. Detail of lung microscopy: multinuclear cells. (HE, original. magnification. 200x).
Figure S2. negative controls of immunohistochemical staining for the ferroptosis marker E06 in myocardium.

Control stains using only secondary antibodies showed no significant signal in the COVID-19 related myocarditis case (Panel A), nor in patients with sudden death due myocarditis of other etiology (Panel B) or the COVID-19 patient without myocarditis (Panel C). Likewise, no significant signal was detected in the myocardium of a control subject without myocarditis or COVID-19 after staining with only the secondary antibody (Panel D).
Figure S3. negative controls of immunohistochemical staining for the ferroptosis markers EO6 and 4-HNE in renal tissue. Staining with only the secondary antibodies from the staining protocols of E06 (Panel A) and anti-4HNE antibody (Panel C) showed a limited signal at the corticomedullary region. In the renal tissue of a case of sudden death due to myocarditis of other etiology a nonspecific signal was detected in the corticomedullary region after staining with these secondary antibodies (Panel B and D).

References

1. Zhu N, Zhang D, Wang W, Zhu N, Zhang D, Wang W, Li X, Yang B, Song J, Zhao X, Huang B, Shi W, Lu R, Niu P. A novel coronavirus from patients with pneumonia in China, 2019. *N Engl J Med* 2020; **382**: 727–733.
2. Guo T, Fan Y, Chen M, Wu X, Zhang L, He T, Wang H, Wan J, Wang X, Lu Z. Cardiovascular implications of fatal outcomes of patients with coronavirus disease 2019 (COVID-19). *JAMA Cardiol* 2020; **5**: 811.
3. Veronese G, Ammirati E, Cipriani M, Frigerio M. Fulminant myocarditis: characteristics, treatment, and outcomes. *Anatol J Cardiol* 2018; **19**: 279–286.
4. Ackermann M, Verleden SE, Kuehnel M, Haverich A, Welte T, Laenger F, Vanstapel A, Werlein C, Stark H, Tzankov A, Li WW, Li VW, Mentzer SJ, Jonigk D. Pulmonary vascular endothelialitis, thrombosis, and angiogenesis in COVID-19. *N Engl J Med* 2020; **383**: 120–128.
5. Corman VM, Landt O, Kaiser M, Molenkamp R, Meijer A, Chu DKW, Bleicker T, Brünink S, Schneider J, Schmidt ML, Mulders DGJC, Haagmans BL, van der Veer B, van den Brink S, Wijsman L, Goderski G, Romette JL, Ellis J, Zambon M, Peiris M, Goossens H, Reusken C, Koopmans MPG, Drosten C. Detection of 2019 novel coronavirus (2019-nCoV) by real-time RT-PCR. *Euro Surveill* 2020; **25**: 2000045.
6. 2019-Novel Coronavirus (2019-nCoV) Real-time rRt-PCR Panel Primers and Probes. 2020. https://www.fda.gov/media/134922/download
7. Bayir H, Anthonymuthu TS, Tyurina YY, Patel SJ, Amoscato AA, Lamade AM, Yang Q, Vladimirov GK, Philpott CC, Kagan VE. Achieving life through death: redox biology of lipid peroxidation in ferroptosis. *Cell Chem Biol* 2020; **27**: 387–408.
8. Horkko S, Bird DA, Miller E, Itabe H, Leitinger N, Subbanagounder G, Berliner JA, Friedman P, Dennis EA, Curtiss LK, Palinski W. Monoclonal autoantibodies specific for oxidized phospholipids or oxidized phospholipid-protein adducts inhibit macrophage uptake of oxidized low-density lipoproteins. *J Clin Invest* 1999; **103**: 117–128.
9. Haider L, Fischer MT, Frischer JM, Bauer J, Hoftberger R, Botond G, Esterbauer H, Binder CJ, Witztum JL, Lassmann H. Oxidative damage in multiple sclerosis lesions. *Brain* 2011; **134**: 1914–1924.
10. Linkermann A, Skouta R, Himmerkus N, Mulay SR, Dewitz C, de Zen F, Prokai A, Zuchtriegel G, Krombach F, Welz PS, Weinlich R, vanden Berghe T, Vandenabeele P, Pasparakis M, Bleich M, Weinberg JM, Reichel CA, Bräsen JH, Kunzendorf U, Anders HJ, Stockwell BR, Green DR, Krautwald S. Synchronized renal tubular cell death involves ferroptosis. *Proc Natl Acad Sci U S A* 2014; **111**: 16836–16841.
11. Feng H, Schorpp K, Jin L, Yozwiak CE, Hoffstrom BG, Decker AM, Rajbhandari P, Stokes ME, Bender HG, Csuka JM, Upadhyayula PS. Transferrin receptor is a specific ferroptosis marker. *Cell Rep* 2020; **30**: 3411, e7–3423.
12. Barton LM, Duval EJ, Stroberg E, Ghosh S, Mukhopadhyay S. COVID-19 autopsies, Oklahoma, USA. *Am J Clin Pathol* 2020; **153**: 725–733.
13. Tian S, Xiong Y, Liu H, Niu L, Guo J, Liao M, Xiao SY. Pathological study of the 2019 novel coronavirus disease (COVID-19) through postmortem core biopsies. *Mod Pathol* 2020; **33**: 1007–1014.
14. Xu Z, Shi L, Wang Y, Zhang J, Huang L, Zhang C, Liu S, Zhao P, Liu H, Zhu L, Tai Y, Bai C, Gao T, Song J, Xia P, Dong J, Zhao J, Wang FS. Pathological findings of COVID-19 associated with acute respiratory distress syndrome. *Lancet Respir Med* 2020; **8**: 420–422.
15. Sala S, Peretto G, Gramegna M, Palmisano A, Villatore A, Vignale D, de Cobelli F, Tresoldi M, Cappelletti AM, Basso C, Godino C, Esposito A. Acute myocarditis presenting as a reverse Tako-Tsubo syndrome in a patient with SARS-CoV-2 respiratory infection. *Eur Heart J* 2020; **41**: 1861–1862.
16. Inciardi RM, Lupi L, Zaccone G, Italia L, Raffo M, Tomasoni D, Cani DS, Cerini M, Farina D, Gavazzi E, Maroldi R. Cardiac involvement in a patient with coronavirus disease 2019 (COVID-19). *JAMA Cardiol* 2020; **5**: 819–824.
17. Tavazzi G, Pellegrini C, Maurelli M, Belliato M, Sciutti F, Bottazzi A, Sepe PA, Resasco T, Camporotondo R, Bruno R, Baldanti F, Paolucci S, Pelenghi S, Iotti GA, Mojoli F, Arbustini E. Myocardial localization of coronavirus in COVID-19 cardiogenic shock. *Eur J Heart Fail* 2020; **22**: 911–915.
18. Escher F, Pietsch H, Aleshcheva G, Bock T, Baumeier C, Elsaesser A, Wenzel P, Hamm C, Westenfeld R, Schultheiss M,

Gross U. Detection of viral SARS-COV-2 genomes and histopathological changes in endomyocardial biopsies. *ESC Heart Failure* 2020. https://doi.org/10.1002/ehf2.12805

19. Caforio AL, Pankuweit S, Arbustini E, Basso C, Gimeno-Blanes J, Felix SB, Fu M, Heliö T, Heymans S, Jahns R, Klingel K. Current state of knowledge on aetiology, diagnosis, management, and therapy of myocarditis: a position statement of the European Society of Cardiology Working Group on Myocardial and Pericardial Diseases. *Eur Heart J* 2013; **34**: 2636–2648d.

20. Hu H, Ma F, Wei X, Fang Y. Coronavirus fulminant myocarditis saved with glucocorticoid and human immunoglobulin. *Eur Heart J* 2020. https://doi.org/10.1093/eurheartj/ehaa190

21. Zeng JH, Liu YX, Yuan J, Wang FX, Wu WB, Li JX, Wang LF, Gao H, Wang Y, Dong CF, Li YJ, Xie XJ, Feng C, Liu L. First case of COVID-19 complicated with fulminant myocarditis: a case report and insights. *Infection* 2020.

22. Dixon SJ, Lemberg KM, Lamprecht MR, Skouta R, Zaitsev EM, Gleason CE, Patel DN, Bauer AJ, Cantley AM, Yang WS, Morrison B III, Stockwell BR. Ferroptosis: an iron-dependent form of nonapoptotic cell death. *Cell* 2012; **149**: 1060–1072.

23. Oudit GY, Kassiri Z, Jiang C, Liu PP, Poutanen SM, Penninger JM, Butany J. SARS-coronavirus modulation of myocardial ACE2 expression and inflammation in patients with SARS. *Eur J Clin Invest* 2009; **39**: 618–625.

24. Imai Y, Kuba K, Neely GG, Yaghubian-Malhami R, Perkmann T, van Loo G, Ermolaeva M, Veldhuizen R, Leung YHC, Wang H, Liu H, Sun Y, Pasparakis M, Kopf M, Mech C, Bavari S, Peiris JSM, Slutsky AS, Akira S, Hultqvist M, Holmdahl R, Nicholls J, Jiang C, Binder CJ, Penninger JM. Identification of oxidative stress and Toll-like receptor 4 signaling as a key pathway of acute lung injury. *Cell* 2008; **133**: 235–249.

25. Chen G, Wu D, Guo W, Cao Y, Huang D, Wang H, Wang T, Zhang X, Chen H, Yu H, Zhang X, Zhang M, Wu S, Song J, Chen T, Han M, Li S, Luo X, Zhao J, Ning Q. Clinical and immunological features of severe and moderate coronavirus disease 2019. *J Clin Invest* 2020; **130**: 2620–2629.

26. Torti FM, Torti SV. Regulation of ferritin genes and protein. *Blood* 2002; **99**: 3505–3516.

27. Rosário C, Zandman-Goddard G, Meyron-Holtz EG, D'Cruz DP, Shoenfeld Y. The hyperferritinemic syndrome: macrophage activation syndrome, Still's disease, septic shock and catastrophic antiphospholipid syndrome. *BMC Med* 2013; **11**: 185.

28. Hassannia B, Wiernicki B, Ingold I, Qu F, van Herck S, Tyurina YY, Bayır H, Abhari BA, Angeli JPF, Choi SM, Meul E, Heyninck K, Declerck K, Chirumamilla CS, Lahtela-Kakkonen M, van Camp G, Krysko DV, Ekert PG, Fulda S, de Geest BG, Conrad M, Kagan VE, vanden Berghe W, Vandenabeele P, vanden Berghe T. Nano-targeted induction of dual ferroptotic mechanisms eradicates high-risk neuroblastoma. *J Clin Invest* 2018; **128**: 3341–3355.

29. Wenzel SE, Tyurina YY, Zhao J, St. Croix CM, Dar HH, Mao G, Tyurin VA, Anthonymuthu TS, Kapralov AA, Amoscato AA, Mikulska-Ruminska K, Shrivastava IH, Kenny EM, Yang Q, Rosenbaum JC, Sparvero LJ, Emlet DR, Wen X, Minami Y, Qu F, Watkins SC, Holman TR, VanDemark AP, Kellum JA, Bahar I, Bayır H, Kagan VE. PEBP1 wardens ferroptosis by enabling lipoxygenase generation of lipid death signals. *Cell* 2017; **171**: 628, e26–641.

30. Devisscher L, Van Coillie S, Hofmans S, Van Rompaey D, Goossens K, Meul E, Maes L, De Winter H, Van Der Veken P, Vandenabeele P, Berghe TV. Discovery of novel, drug-like ferroptosis inhibitors with in vivo efficacy. *J Med Chem* 2018; **61**: 10126–10140.